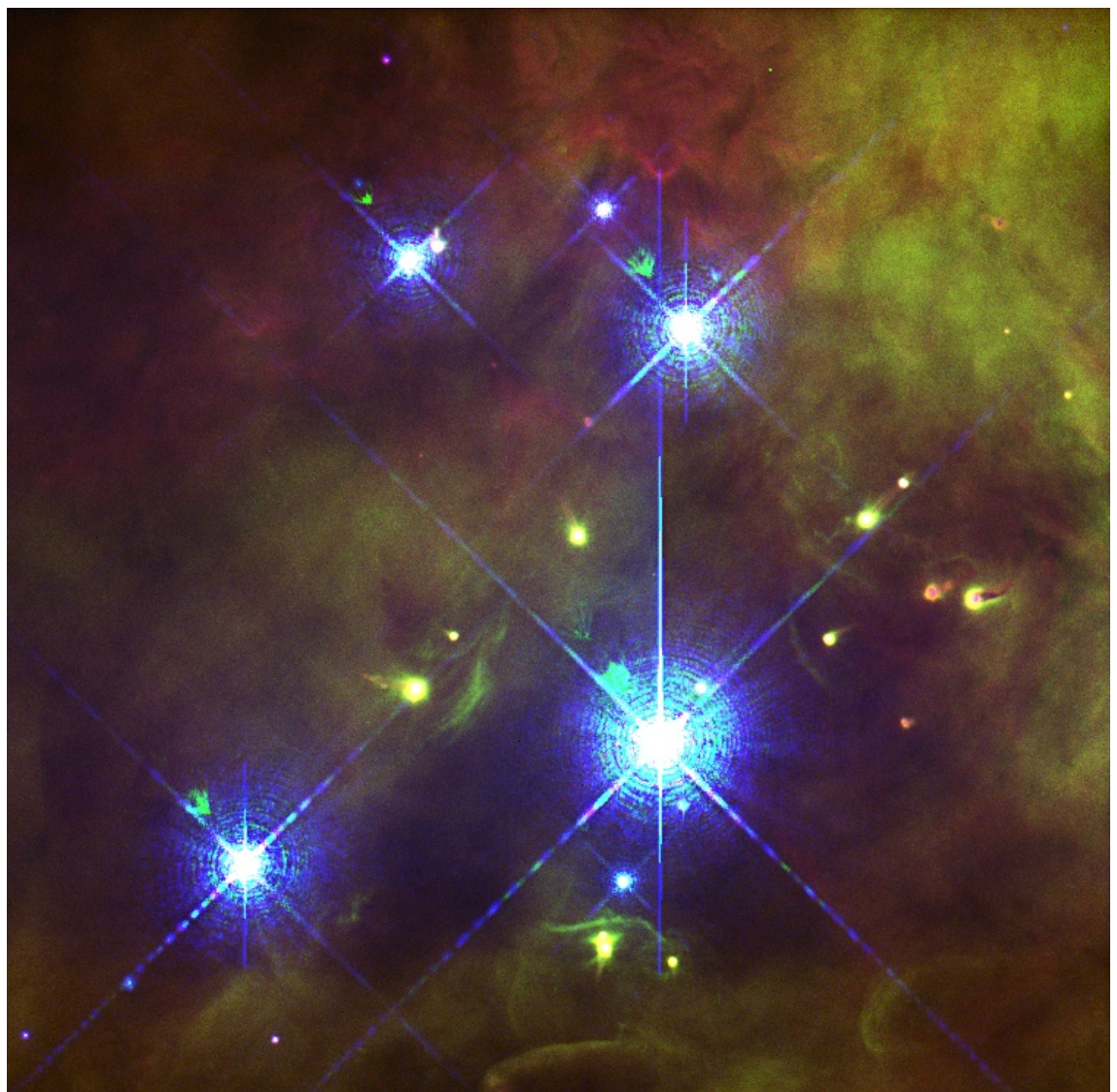


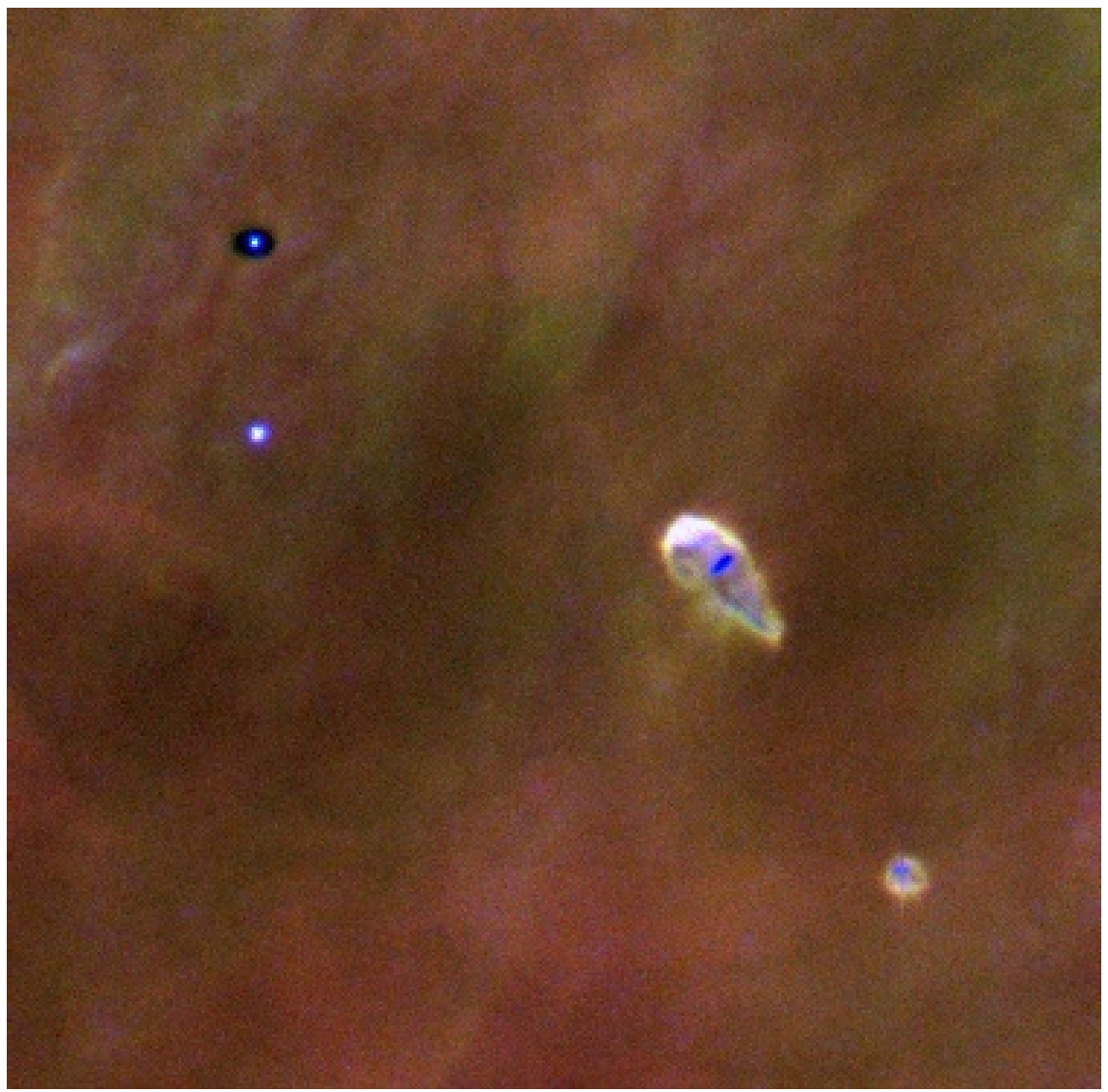
3D Resonance Line Transfer in Moving Media

Bredbeck Workshop, 07. - 10. July 2003

Dr. Erik Meinköhn
Institut für Theoretische Astrophysik
and
Institut für Angewandte Mathematik – Numerik
Heidelberg University
Germany



Hubble-Space-Telescope-Photo of the center of the Orion nebula. The four bright stars illuminate the nebula and reveal a very inhomogenous and star forming surrounding medium. The comet type objects are so-called Young Stellar Objects (YSO).



A closeup view of a Young Stellar Object illuminated by a central star of the Orion nebula.

Contents

- Introduction
- Monochromatic 3D Radiative Transfer
 - Problem Definition
 - Finite Element Method (FEM)
 - Error Estimation and Adaptivity
- Polychromatic 3D Line Transfer
 - Problem Definition
 - Physical Assumptions
 - Finite Element Discretization

Introduction Radiative Transfer

Important for:

- spectral diagnostics
 - coupling to hydrodynamics ("radiation-hydrodynamics")

In astrophysics:

- radiation fields are specified by specific intensity

$$I = I(\mathbf{x}, \mathbf{n}, \mathbf{v}, t, p)$$

- I is determined by radiative transfer equation

$$\frac{dI}{ds} = -\chi I + \eta$$





 creation by
 “scattering” from
 thermal pool

Monochromatic 3D Radiative Transfer

$$\mathbf{n} \cdot \nabla_x I(\mathbf{x}, \mathbf{n}) + (\kappa(\mathbf{x}) + \sigma(\mathbf{x})) I(\mathbf{x}, \mathbf{n})$$

$$- \frac{\sigma(\mathbf{x})}{4\pi} \int_{S^2} P(\mathbf{n}', \mathbf{n}) I(\mathbf{x}, \mathbf{n}') d\omega' = f(\mathbf{x}),$$

in $\Omega \subset R^3$

$I(\mathbf{x}, \mathbf{n})$... specific intensity

$\kappa(\mathbf{x})$... absorption coefficient

$\sigma(\mathbf{x})$... scattering coefficient

$f(\mathbf{x})$... source function

$P(\mathbf{n}', \mathbf{n})$... phase function

S^2 ... unit sphere in R^3

\mathbf{n} ... unit vector on S^2

Boundary conditions:

$$I(\mathbf{x}, \mathbf{n}) = g(\mathbf{x}, \mathbf{n}) \quad \text{on} \quad \Gamma_- = \{(\mathbf{x}, \mathbf{n}) \in \Gamma | \mathbf{n}_\Gamma \cdot \mathbf{n} < 0\}$$

For abbreviation we use the operator form of the radiative transfer equation:

$$\mathbf{n} \cdot \nabla_x I + (\kappa + \sigma) I - \frac{\sigma}{4\pi} \int_{S^2} P(\mathbf{n}', \mathbf{n}) I(\mathbf{x}, \mathbf{n}') d\omega' = \mathcal{A}I = f$$

Unpleasant features when treating numerically:

- high dimension (5D)
- κ and σ vary strongly in space (steep gradients)
- ill-conditioned transport matrix for scattering dominated problems and large optical depth $\tau = \int \chi(\mathbf{x}) ds = \int (\kappa(\mathbf{x}) + \sigma(\mathbf{x})) ds$



Make the use of
supercomputers
indispensable

Example:

- using a reasonable resolution in space $h = \frac{1}{1000}$
- 1000 ray directions (ordinates)

$\implies 10^{12}$ unknown for 3D geometry

Conclusions:

application of efficient error estimation and grid adaption techniques
in combination with
parallelization strategies is necessary to obtain reliable quantitative results

Finite Element Method (FEM)

- natural space for finding solutions of the monochromatic RTE:

$$W = \{ I \in L^2(\Omega \times S^2) \mid \mathbf{n} \cdot \nabla_x I \in L^2(\Omega \times S^2) \}$$

- usually we use homogeneous vacuum boundary conditions (i.e. $g(\mathbf{x}, \mathbf{n}) = 0$)

$$\implies W_0 = \{ I \in W \mid I = 0 \text{ on } \Gamma_- \}$$

- weak formulation: Find $I \in W_0$, such that
 $\forall \varphi \in W_0$

$$\begin{aligned} & \int_{\Omega} \int_{S^2} f(\mathbf{x}) \varphi(\mathbf{x}, \mathbf{n}) d\omega d^3x = \\ & \quad \int_{\Omega} \int_{S^2} \mathbf{n} \cdot \nabla_x I(\mathbf{x}, \mathbf{n}) \varphi(\mathbf{x}, \mathbf{n}) d\omega d^3x \\ & \quad + \int_{\Omega} \int_{S^2} (\kappa(\mathbf{x}) + \sigma(\mathbf{x})) I(\mathbf{x}, \mathbf{n}) \varphi(\mathbf{x}, \mathbf{n}) d\omega d^3x \\ & \quad - \int_{\Omega} \int_{S^2} \int_{S^2} \sigma(\mathbf{x}) P(\mathbf{n}', \mathbf{n}) I(\mathbf{x}, \mathbf{n}') \varphi(\mathbf{x}, \mathbf{n}) d\omega' d\omega d^3x \end{aligned}$$

- extending the definition of the L^2 -scalar product

$$(I, \varphi) = (I, \varphi)_{\Omega \times S^2} = \int_{\Omega} \int_{S^2} I \varphi d\omega d^3x,$$

$$\implies (\mathcal{A}I, \varphi) = (f, \varphi) \quad \forall \varphi \in W_0$$

- stabilization via streamline diffusion modification

$$(\mathcal{A}I, \varphi + \delta \mathbf{n} \cdot \nabla_x \varphi) = (f, \varphi + \delta \mathbf{n} \cdot \nabla_x \varphi) \quad \forall \varphi \in W_0.$$

- the discrete analogue

$$(\mathcal{A}I_h, \varphi_h) = (f, \varphi_h) \quad \forall \varphi_h \in W_h.$$

- ordinate discretization:

- on S^2 we use fixed discretization based on refined icosahedron
- constant trialfunctions (seven-dimensional integration)
- second order accurate due to superconvergence

- spatial discretization

- locally refined hexahedral mesh
- continuous piecewise trilinear trialfunctions

Error Estimation and Adaptivity

Aim:

- compare simulations quantitatively with observations
- application of grid adaption technique based on local error indicators

Construction of an a posteriori error estimator:

- suppose, $z(\mathbf{x}, \mathbf{n})$ is the solution of the dual problem

$$\mathcal{M}(\varphi) = (\varphi, \mathcal{A}^* z) \quad \forall \varphi \in W_0 \quad (1)$$

- dual radiative transfer operator is defined by

$$\begin{aligned} \mathcal{A}^* z(\mathbf{x}, \mathbf{n}) &= -\mathbf{n} \cdot \nabla_x z(\mathbf{x}, \mathbf{n}) + (\kappa(\mathbf{x}) + \sigma(\mathbf{x})) z(\mathbf{x}, \mathbf{n}) \\ &\quad - \sigma(\mathbf{x}) \int_{S^2} P(\mathbf{n}', \mathbf{n}) z(\mathbf{x}, \mathbf{n}') d\omega' \end{aligned}$$

boundary condition:

$$I = 0 \quad \text{on} \quad \Gamma_+ = \{(\mathbf{x}, \mathbf{n}) \in \Gamma \mid \mathbf{n}_\Gamma \cdot \mathbf{n} > 0\}$$

- $\mathcal{M}(I) - \mathcal{M}(I_h) = \mathcal{M}(I - I_h) = \mathcal{M}(e)$ is a linear functional corresponding to the measured quantity

Error representation:

$$\begin{aligned}
\mathcal{M}(e) &= (e, \mathcal{A}^* z) \\
&= (\mathcal{A}e, z) \\
&= (\mathcal{A}e, z - z_i) \\
&= \sum_{K \in \mathbb{T}_h} (f - \mathcal{A}I_h, z - z_i)_K \quad \text{for arbitrary } z_i \in W_h
\end{aligned}$$

- using the **Galerkin orthogonality**

$$(\mathcal{A}I - \mathcal{A}I_h, \varphi_h) = 0 \quad \forall \varphi_h \in W_h$$

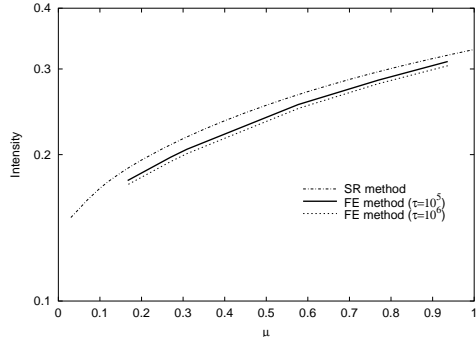
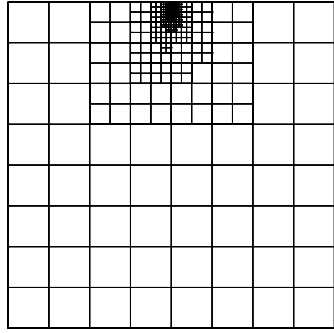
- apply Hölder's inequality and standard approximation estimates of finite element spaces to obtain the estimate

$$\begin{aligned}
\mathcal{M}(e) &\leq \eta = \sum_{K \in \mathbb{T}_h} \eta_K \\
\eta_K &= C_K h_K^2 \|f - \mathcal{A}I_h\|_K \|\nabla^2 z\|_K,
\end{aligned}$$

Examples of error functionals:

- **L^2 -error:** $\mathcal{M}(\varphi) := \|e\|^{-1} (e, \varphi) \rightarrow \mathcal{M}(e) = \|e\|$
- **point error:** $\mathcal{M}(\varphi) = \varphi(\mathbf{x}_0, \mathbf{n}_0) \rightarrow \mathcal{M}(e) = e(\mathbf{x}_0, \mathbf{n}_0)$
- **flux error:**

$$\mathcal{M}(\varphi) = \int_{\Gamma_{\text{obs}}} \varphi(\mathbf{x}, \mathbf{n}_{\text{obs}}) \mathbf{n}_{\Gamma} \cdot \mathbf{n}_{\text{obs}} dx$$



Angular distribution of the specific intensity $I(\mathbf{x}_0, \mu)$ leaving the slab from a boundary point \mathbf{x}_0 for large optical depths $\tau = 10^5, 10^6$ and albedo $\gamma = 0.98$ (right) and the corresponding locally refined grid (left).

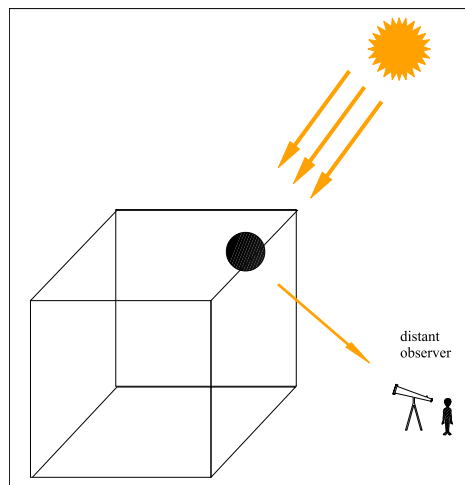
FE				FD			
DUAL		L2		GLOBAL		GLOBAL	
vertices	value	vertices	value	vertices	value	vertices	value
125	0.427	125	0.427	125	0.427	35 937	0.576
501	0.596	579	0.525	729	0.591	274 625	0.616
2 213	0.661	2 474	0.640	4 913	0.642	2 146 689	0.642
8 103	0.672	10 935	0.662	35 937	0.661		
14 953	0.674	86 903	0.669	274 625	0.669		

Quantitative analysis of the specific Intensity $I(\mathbf{x}_0, \mathbf{n}_0)$ leaving the slab from a boundary point \mathbf{x}_0 in a particular direction $\mathbf{n}_0 = 0.705$ for two adaptively refined (L2,DUAL) and an unstructured grid (GLOBAL). The optical depth and the albedo is $\tau = 20$ and $\gamma = 0.8$, respectively.

$\tau = 0.4$						
	FE					FD
# processors	1	2	4	8	16	1
memory [MB]	31.9	16.7	9.0	5.2	3.3	13
CPU time [s]	846.5	371.8	121.4	56.2	48.2	1275.0
$\tau = 20$						
	FE					FD
# processors	1	2	4	8	16	1
memory [MB]	196	99.6	52.2	28.7	15.1	99
CPU time [s]	3167.2	1364.2	428.7	207.1	136.1	9878.9

Comparison of the memory and CPU requirements of the three-dimensional codes for modeling an optical thick and an optical thin plan-parallel layer. The albedo is $\gamma = 0.80$ in both cases. The FE method employs the DUAL grid refinement strategy. The final grid has 670 and 4263 vertices for the optical thin and thick case, respectively. The FD code uses a structured grid (GLOBAL) with 65^3 vertices for $\tau = 0.4$ and 129^3 vertices for $\tau = 20$. In the latter case, the resolution of the spatial grid is too low to obtain a solution as accurate as for the FE code.

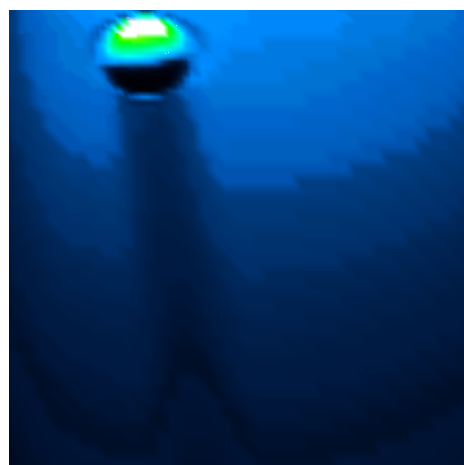
Simulation and Visualization of a Young Stellar Object (YSO)



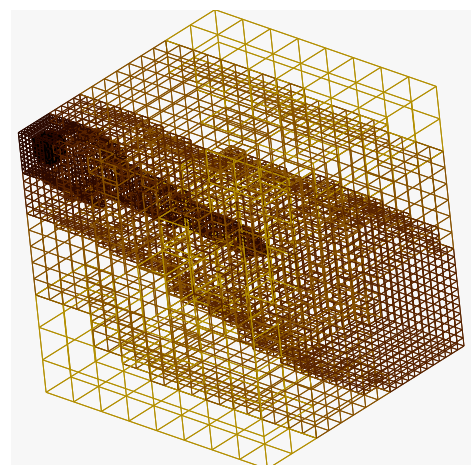
model configuration



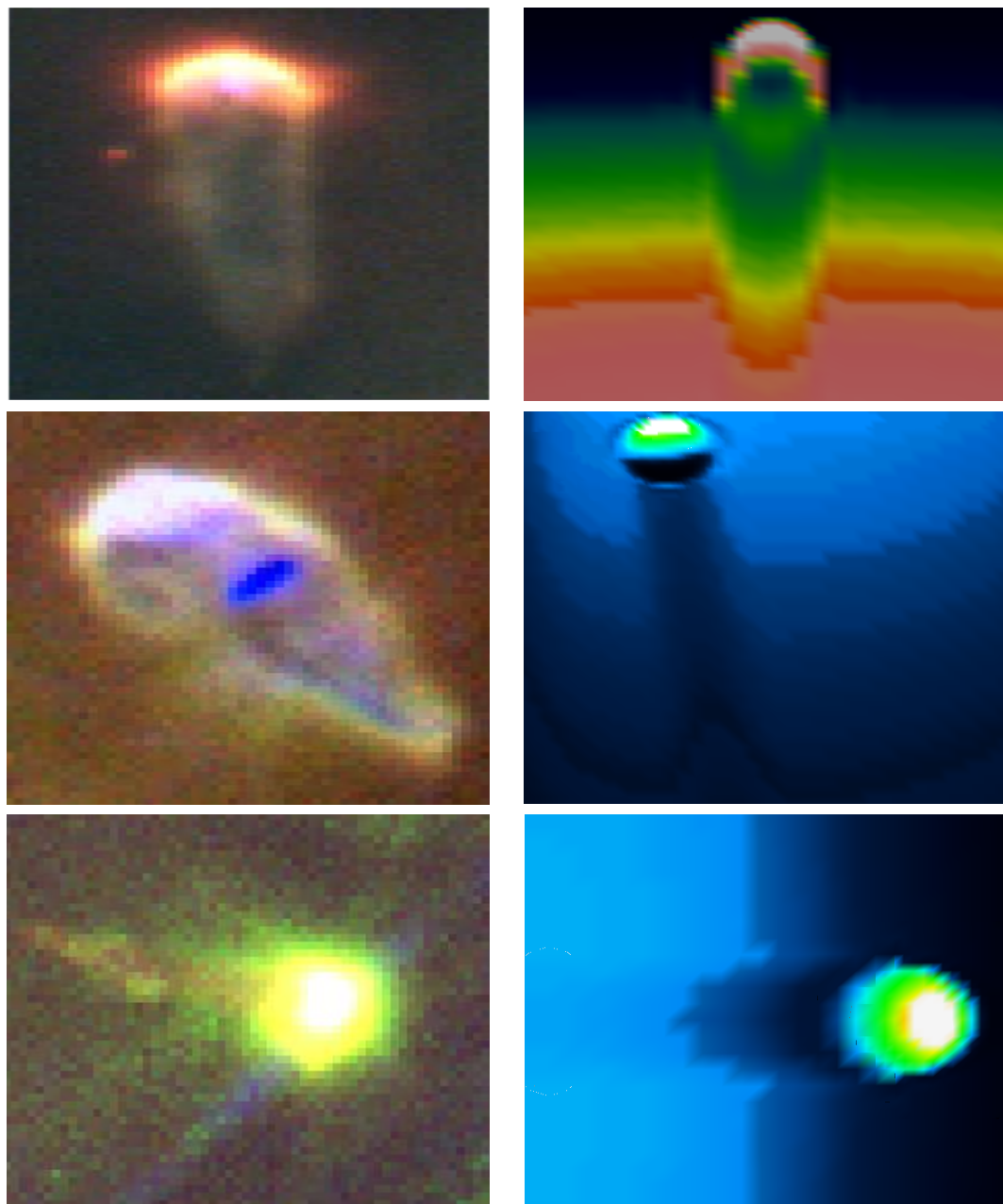
Hubble-Space-Telescope-Photo



visualization of a simulated YSO



locally refined 3D grid



The left row shows three Hubble-Space-Telescope photos of YSOs being illuminated by the central stars of the Orion nebula. The right row displays the visualization of a simulated 3D radiation field of an illuminated YSO from three different viewing angles.

Polychromatic 3D Line Transfer

$$(\mathcal{T} + \mathcal{D} + \mathcal{S} + \chi(\mathbf{x}, \mathbf{v})) I(\mathbf{x}, \mathbf{n}, \mathbf{v}) = f(\mathbf{x}, \mathbf{v})$$

The transfer operator \mathcal{T} , the “Doppler” operator \mathcal{D} , and the scattering operator \mathcal{S} are defined by

$$\mathcal{T} I(\mathbf{x}, \mathbf{n}, \mathbf{v}) = \mathbf{n} \cdot \nabla_x I(\mathbf{x}, \mathbf{n}, \mathbf{v})$$

$$\mathcal{D} I(\mathbf{x}, \mathbf{n}, \mathbf{v}) = w(\mathbf{x}, \mathbf{n}) \mathbf{v} \frac{\partial}{\partial \mathbf{v}} I(\mathbf{x}, \mathbf{n}, \mathbf{v})$$

$$\mathcal{S} I(\mathbf{x}, \mathbf{n}, \mathbf{v}) = -\frac{\sigma(\mathbf{x})}{4\pi} \int_0^\infty \int_{S^2} R(\hat{\mathbf{n}}, \hat{\mathbf{v}}; \mathbf{n}, \mathbf{v}) I(\mathbf{x}, \hat{\mathbf{n}}, \hat{\mathbf{v}}) d\hat{\omega} d\hat{\mathbf{v}}$$

$I(\mathbf{x}, \mathbf{n}, \mathbf{v})$... invariant intensity

$w(\mathbf{x}, \mathbf{n})$... gradient of velocity field
in direction \mathbf{n}

$R(\hat{\mathbf{n}}, \hat{\mathbf{v}}; \mathbf{n}, \mathbf{v})$... redistribution function

$\chi(\mathbf{x}, \mathbf{v}) = \kappa(\mathbf{x}, \mathbf{v}) + \sigma(\mathbf{x}, \mathbf{v})$... opacity

$\kappa(\mathbf{x}, \mathbf{v}) = \kappa(\mathbf{x}) \Phi(\mathbf{v})$... absorption coefficient

$\sigma(\mathbf{x}, \mathbf{v}) = \sigma(\mathbf{x}) \Phi(\mathbf{v})$... scattering coefficient

$\Phi(\mathbf{v})$... normalized line profile function

Physical Assumptions

- Doppler profile function:

$$\Phi(v) = \frac{1}{\sqrt{\pi} \Delta v_D} \exp \left[- \left(\frac{v - v_c}{\Delta v_D} \right)^2 \right]$$

- source term:

$$f(\mathbf{x}, v) = \kappa(\mathbf{x}, v) B(T(\mathbf{x}), v) + \varepsilon(\mathbf{x}, v)$$

- gradient of the Velocity field $\mathbf{v}(\mathbf{x})$ in direction \mathbf{n} :

$$w(\mathbf{x}, \mathbf{n}) = -\mathbf{n} \cdot \nabla_x \left(\mathbf{n} \cdot \frac{\mathbf{v}(\mathbf{x})}{c} \right)$$

- using an angle-averaged redistribution function

$$R(\hat{v}, v) = \frac{1}{(4\pi)^2} \int_{S^2} \int_{S^2} R(\mathbf{x}, \hat{\mathbf{n}}, \hat{v}; \mathbf{n}, v) d\hat{\omega} d\omega,$$

we rewrite the scattering operator

$$SI = -\frac{\sigma(\mathbf{x})}{4\pi} \int_0^\infty R(\hat{v}, v) \int_{S^2} I(\mathbf{x}, \hat{\mathbf{n}}, \hat{v}) d\hat{\omega} d\hat{v}$$

Examples of angle-averaged redistribution functions:

(a) coherent scattering

$$R(\hat{v}, v) = \Phi(\hat{v}) \delta(v - \hat{v})$$

(b) complete redistribution

$$R(\hat{v}, v) = \Phi(\hat{v}) \Phi(v)$$

Boundary Conditions:

$$I(\mathbf{x}, \mathbf{n}, v) = I_{\text{cont}}(\mathbf{x}, \mathbf{n}, v) \quad \text{on } \Sigma^- = \Omega \times S^2 \times \partial\Lambda$$

$$I(\mathbf{x}, \mathbf{n}, v) = g(\mathbf{x}, \mathbf{n}, v) \quad \text{on } \Gamma^- \times \Lambda = \{ I(\mathbf{x}, \mathbf{n}, v) \in \Gamma \mid \mathbf{n}_\Gamma \cdot \mathbf{n} < 0 \}$$

For the modelling of prominent resonance lines we restrict the frequency space to a finite intervall:

$$\Lambda := [v_{\text{lower}}, v_{\text{upper}}]$$

Discretization:

discontinuous Galerkin method (DG(0)) for additional frequency derivative

$$w(\mathbf{x}, \mathbf{n}) v \frac{\partial I}{\partial v} \longrightarrow w v_i \frac{I_i - I_{i-1}}{\Delta v} \quad (w_i > 0)$$

and

$$w(\mathbf{x}, \mathbf{n}) v \frac{\partial I}{\partial v} \longrightarrow w v_i \frac{I_{i+1} - I_i}{\Delta v} \quad (w_i < 0)$$

↔
 implicite Euler-technique for N
 equidistantly distributed frequency
 points
 $v_i \in \{v_{\text{lower}} = v_1, v_2, \dots, v_N = v_{\text{upper}}\} \subset \Lambda$

- separating the unknown quantities I_i from the known quantities I_j , the semi-discrete scattering operator reads

$$\frac{\sigma_i}{4\pi} \Phi_i q_i \int_{S^2} I_i d\hat{\omega} + \frac{\sigma_i}{4\pi} \sum_{j \neq i}^N \Phi_j q_j \int_{S^2} I(\mathbf{x}, \hat{\mathbf{n}}, \mathbf{v}_j) d\hat{\omega}.$$

- semi-discrete formulation of the line transfer problem for each frequency point \mathbf{v}_i

$$\begin{aligned} \mathcal{A}_i^{\text{crd}} I_i &= \hat{f}_i \\ &\Updownarrow \\ \left(\mathcal{A}_i^{\text{mono}} + \frac{|w| \mathbf{v}_i}{\Delta \mathbf{v}} \right) I_i &= \tilde{f}_i + \frac{\sigma_i}{4\pi} \sum_{j \neq i}^N \Phi_j q_j \int_{S^2} I(\mathbf{x}, \hat{\mathbf{n}}, \mathbf{v}_j) d\hat{\omega}, \end{aligned} \quad (2)$$

where

$$\mathcal{A}_i^{\text{mono}} = \mathcal{T} + \chi_i + \Phi_i q_i \mathcal{S}^{\text{coh}}$$

$$\tilde{f}_i = f_i + \frac{|w| \mathbf{v}_i}{\Delta \mathbf{v}} \begin{cases} I_{i-1} & (w > 0) \\ I_{i+1} & (w < 0) \end{cases}$$

- total discrete system has the matrix form:

$$\begin{pmatrix} \mathbf{A}_1^{\text{crd}} & \mathbf{R}_1 + \mathbf{Q}_2 & \mathbf{Q}_3 & \dots & \mathbf{Q}_N \\ \mathbf{B}_2 + \mathbf{Q}_1 & \mathbf{A}_2^{\text{crd}} & \mathbf{R}_2 + \mathbf{Q}_3 & \ddots & \vdots \\ \mathbf{Q}_1 & \ddots & \ddots & \ddots & \vdots \\ \vdots & \ddots & \ddots & \ddots & \vdots \\ \mathbf{Q}_1 & \dots & \dots & \dots & \mathbf{A}_N^{\text{crd}} \end{pmatrix} \begin{pmatrix} \mathbf{I}_1 \\ \mathbf{I}_2 \\ \vdots \\ \vdots \\ \mathbf{I}_N \end{pmatrix} = \begin{pmatrix} \hat{\mathbf{f}}_1 \\ \hat{\mathbf{f}}_2 \\ \vdots \\ \vdots \\ \hat{\mathbf{f}}_N \end{pmatrix}$$

Full Solution Algorithm:

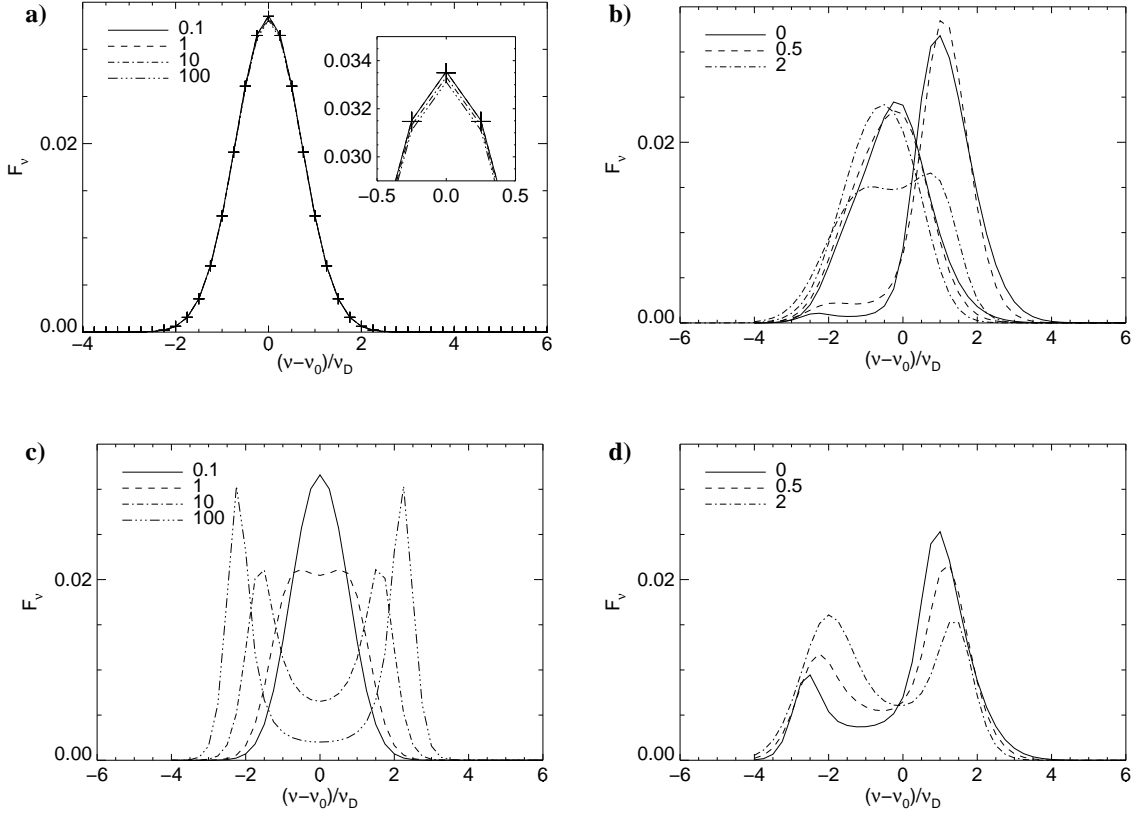
1. Start with $I_i = 0$ for all frequencies v_i
2. Solve Eq. (2) for $i = 1, \dots, N$
3. use solution as start value for the next solution step (Block-Gauss-Seidel)
4. Repeat step 2 and 3 until convergence is reached
5. Refine grid and repeat step 2–4

Pro:

- Block-Gauss-Seidel technique allows for very good resolution in the spatial, ordinate and the frequency domain

Contra:

- fix point iteration
- ill-conditioned transport matrix for dominant scattering ($\sigma(x, v) \gg 1$) and large optical depths
- error indicator is not sharp ($\eta_K = \max(\eta_K(v_i)|_{v_i})$)



Ly α line profiles calculated with the FE code for a spherically symmetric model configuration: a) a static halo with coherent scattering, b) an infalling halo with coherent scattering, c) a static halo with complete redistribution, and d) an infalling halo with complete redistribution. For the static cases a) and c) the line styles refer to calculations with different optical depth τ as indicated. The small window in a) enlarges the peak of the line. The crosses mark the results of the analytical solution. For the moving halos we show in b) the results for $\tau = 1$ (thin lines) and $\tau = 10$ (thick lines) and in d) only for $\tau = 10$. Here, the line styles refer to the exponent l used for the velocity fields.